Effect of Acidity and Manner of Addition of HZSM-5 Catalyst on the Aromatic Products during Catalytic Upgrading of Biomass Pyrolysis

Yunwu Zheng,[a,b] Lei Tao,[b] Xiaoqin Yang,[a] Yuanbo Huang,[a] Can Liu,[a] Jiyou Gu,[b,*] and Zhifeng Zheng [a,*]

To investigate the effects of acidity on aromatic yield and selectivity during the catalytic pyrolysis of biomass, the silica to alumina ratio (SAR), as well as the amount and addition method of HZSM-5 catalyst were varied. The results showed that with an increase in the SAR, the pore volume was reduced, the average pore diameter of the HZSM-5 catalyst increased, and the total acidity and catalytic activity decreased. Meanwhile, the increase in acidity led to an increased non-condensable gases yield, which was associated with a decrease in the bio-oil yield. The calorific value and moisture content increased, and the ability of deoxygenation was enhanced. The single ring aromatic hydrocarbons (BTXE) content increased, and the polycyclic aromatic hydrocarbons (2-ring, 3-ring) content decreased noticeably. The selectivity of BTXE decreased substantially from 69 wt.% to 6.85 wt.%, while the selectivity of naphthalene and its derivatives increased remarkably, as the SAR increased. Additionally, the acidity increased the selectivity of unsubstituted aromatic compounds, but decreased the selectivity of substituted aromatic compounds. Moreover, *ex situ* catalytic pyrolysis more effectively enhanced the aromatic hydrocarbon yield and selectivity (69 wt.%) compared with *in situ* catalytic pyrolysis (27.51 wt.%), and *in situ* catalytic pyrolysis generated more polyaromatics and solid residue.

Keywords: Biomass pyrolysis; Catalytic pyrolysis upgrading; Acidity; Addition ways; HZSM-5 catalyst

Contact information: a: Yunnan Provincial Key Laboratory of Wood Adhesives and Glued Products, Yunnan Province, University Key Laboratory of Biomass Chemical Refinery & Synthesis, Yunnan Province, College of Materials Engineering, Southwest Forestry University, Kunming 650224, China; b: Key Laboratory of Bio-based Material Science & Technology, Ministry of Education, College of Materials Science and Engineering, Northeast Forestry University, Harbin 150040, China;
**Corresponding authors: biomass_x@163.com, zhengzhifeng666@163.com*

INTRODUCTION

Light aromatic hydrocarbons, such as benzene, toluene, xylene, and naphthalene (BTXE), are basic organic chemical raw materials that are widely used in plastics, pesticides, pharmaceuticals, and the fuel industry. At present, these aromatic hydrocarbons mainly come from fossil fuels. However, it is well known that fossil fuel reserves are in the process of being depleted. The shortage of this raw material is a main factor that affects the production of SO_x and NO_x emissions, which are released from the process of the transformation and utilization of fossil fuels and pollute the environment. Therefore, broadening the sources of raw materials and finding the right renewable raw materials to replace non-renewable oil for producing BTXE is important. Biomass is a plant resource that is composed of organic carbon, and it is the only renewable resource

that can be used to produce liquid fuels at present. It is also the most extensive source of raw materials. Therefore, biomass has great potential for use as a raw material for the preparation of aromatic chemicals.

The bio-oil produced from traditional biomass by pyrolysis has a high oxygen content, high water content, high viscosity, strong acidity, strong instability, and is not compatible with traditional liquid fuel, which limits its applications (Huber *et al*. 2006; Kunkes *et al*. 2008). The introduction of appropriate catalysts for catalytic pyrolysis to improve the quality of the resultant oil is key to improve this alternative raw material, and it is also a popular topic of research for biomass energy (Jae *et al*. 2014). At present, ZSM-5 is considered to be an ideal catalyst in the field of biomass catalytic pyrolysis because of its strong surface acidity and unique pore structure. It is capable of breaking chemical bonds, achieving shape-selectivity with respect to reaction products, as well as undergoing reactions to deoxygenate and aromatization. It can effectively reduce the content of oxygenated compounds in bio-oil, while increasing the relative content of hydrocarbons (Carlson *et al*. 2009; Zhang *et al*. 2013). The higher catalytic performance of ZSM-5 is mainly due to its strong and unique pore structure. Changing the SiO_2 to Al_2O_3 ratio (SAR) did not affect the overall structure of the catalyst. The acid strength and acid site density, which affected the activity of the catalyst, deactivated the catalyst and affected the quality and distribution of the products (Haw 2002).

Mukarakate *et al*. (2014) upgraded pine pyrolysis vapors using β-zeolite with widely varying SARs. Here, the cited authors demonstrated that decreasing the SAR (increasing number of acid sites) led to an increase in the coke deposition and aromatic upgraded vapor yield. Foster *et al*. (2012) found that the distribution of aromatic hydrocarbon products from glucose pyrolysis changed slightly between samples. The ZSM-5 sample with the highest aluminum content showed the highest selectivity towards smaller aromatic products (benzene and toluene), and samples with a lower amount of aluminum were slightly more selective towards larger products ($C8^+$ aromatics and polyaromatics). The larger aromatic products included xylenes, ethylbenzene, trimethylbenzene, ethylmethyl benzene, and indane. The optimum aluminum content of the ZSM-5 CFP catalyst to maximize yield of aromatic hydrocarbons occurs at a SAR of 30. Murata *et al*. (2012) used jatropha wastes (husk, seed shell, and branch) as materials, and they found that the selectivity to aromatic compounds in H-ZSM-5 with different Si/Al_2ratio was similar. But, in USY, aromatic selectivity was USY(6.3) > USY(14) > USY(360). In the materials with medium-size pore structure including H-ZSM-5, the aromatic selectivity was H-ZSM-5(280)> ZSM-11(480)> FER(20). Shen *et al*. (2016) studied the catalytic pyrolysis of two lignin samples extracted from Chinese fir and rice straw by pyrolysis-gas chromatography/mass spectrometry (Py-GC/MS), concerning the effect of reaction temperatures (550 to 900 °C) and catalyst species (HZSM-5 (25), HZSM-5 (50), HZSM-5 (210), H-b, and H-USY) on the production of specific aromatic hydrocarbons (such as benzene, toluene, and xylene) showed that the yield of specific aromatic hydrocarbons from catalytic pyrolysis of the two lignin samples with HZSM-5 (25) achieved the maximum value at 650 °C. Formation of p-xylene was remarkably promoted with the decreased Si/Al ratio of HZSM-5 over that of toluene.

Most papers have focused on the yields and selectivity of aromatic hydrocarbon with traditional manner, and there has been relatively little attention paid to the structure, properties of bio-oil, and the lifetime of the catalyst. At the same time, the effect on the yields and selectivity of aromatic hydrocarbons from upgrading catalytic pyrolysis of biomass with HZSM-5 as a function of the acidity and catalyst addition manner has not

been fully investigated. This study investigated the effect of the acid sites, catalyst amount, and catalyst addition manner on the products distribution from catalytic pyrolysis of Yunnan pine with novel statistical methods, and HZSM-5 catalysts with different SARs (25, 38, 50, and 280) were employed. The biomass to catalyst ratios were 1:1, 1:2, 1:3, and 1:5. The physical and chemical properties, such as the mass fraction of oxygen, hydrocarbon ratio and calorific value, chemical structure, and selectivity of aromatics, was used to estimate the activity of the catalyst. The lifetime of catalyst and bio-oil characteristics were also evaluated. The results provided a reference for the preparation of the catalyst and improvement of the bio-oil quality, and opened up a new path for the development and utilization of aromatic compounds produced from biomass.

EXPERIMENTAL

Materials

The Yunnan pine used in this study was collected from Pu'er city in Yunnan Province, China. Prior to the experiments, the Yunnan pine particles were sieved to a particle size of 0.250 mm to 0.420 mm. The feedstock was dried at 105 °C ± 2 °C until it reached a constant weight, and it was then sealed in bags. The main characteristics of Yunnan pine are listed in Table 1. The proximate analysis of Yunnan pine was conducted on a TG 209 F3 Tarsus (NETZSCH-Gerätebau GmbH, Bavarian State Germany). The moisture, ash, and volatile compounds contents were identified using the ASTM standards ASTM E871 (1982), E1755 (2001), and ASTM E872 (1998), respectively. The fixed carbon content was calculated by the difference. An EA 1108 elemental analyzer (Elementar, Langenselbold, Germany) was used to conduct the ultimate analysis of Yunnan pine. The cellulose, hemicellulose, and lignin contents were determined according to the method of structural carbohydrates and lignin determination in biomass, which was provided by the National Renewable Energy Laboratory (Sluiter *et al.* 2008). Tetrahydrofuran AR was provided by Tianjin Zhiyuan Chemical Reagent Company (Nanjing, China). High-purity nitrogen was provided by Kunming Messer Company (Kunming, China).

Table 1. Proximate, Ultimate, and Component Analyses of Yunnan Pine

Proximate Analysis (wt.%)	Moisture[a]	2.12 ± 0.17
	Volatile Compounds[a]	83.22 ± 0.98
	Fixed Carbon[a]	13.45 ± 0.42
	Ash[a]	1.21 ± 0.08
	C	49.66 ± 0.43
	H	8.23 ± 0.59
	N	0.21 ± 0.03
	S	0.13 ± 0.05
	O[b]	41.77 ± 0.51
	Cellulose	44.39 ± 0.52
	Hemicellulose	24.16 ± 0.83
	Lignin	31.45 ± 0.46

[a] Air-dry basis; [b] By difference

The HZSM-5 molecular sieve catalyst with a white bar structure was obtained from the Catalyst Plant of Nankai University (Nanjing, China). The SAR of ZSM-5 was approximately 25. The chemical composition of the catalysts was as follows: Al_2O_3, 5 wt.% to 5.5 wt.%; SiO_2, 80 wt.% to 85 wt.%. The absorption capacities of hexane, cyclohexane, and water were 9.5 wt.% to 10.5 wt.%, 2.0 wt.% to 2.5 wt.%, and 11.0 wt.% to 12.0 wt.%, respectively. Before the experiment, the HZSM-5 was ground manually in a mortar until it could pass through a 0.185- to 0.250-mm sieve.

In this synthesis, sodium silicate was used as silica source, and sodium hydroxide was slowly added to this solution followed by the addition of aluminum nitrate and tetra-propyl ammonium hydroxide (TPAOH). The components were mixed with constant stirring at room temperature. The pH of the resulting gel was then adjusted to 10.5 by adding 1:1 H_2SO_4 solution before charging it in Teflon lined autoclave for hydrothermal synthesis at 180 °C for 3 days. The resultant powder obtained was thoroughly washed with ample amount of water to remove any residual ions left on the material. The Na-form of zeolite thus obtained has been refluxed with 5 N ammonium nitrate solution three times followed by its calcination so as to obtain the proton form of ZSM-5. The main purpose of calcinations is to remove the organic template (TPAOH) by decomposition, leaving the micropores in the zeolite. Throughout this process the mole ratio of silica source and aluminum nitrate was varied to obtain catalysts with different SiO_2/Al_2O_3 ratios.

The catalyst samples were dried in a high temperature carbonization furnace at a temperature of 500 °C and activated for 4 h. The samples were then cooled using 0.5 mol/mL NH_4NO_3 solution impregnation (quality ratio: 1 g:100 mL) with a reaction temperature of 80 °C and reaction time of 2 h. Afterwards, the samples were filtered, washed, dried at 105 °C for 12 h, and then calcined at 500 °C for 4 h. The samples were cooled, and the above steps were repeated (Wei *et al*. 2011). The samples were named according to the SAR (SAR25, SAR38, SAR50, and SAR280), and then sealed for the experiment.

Methods

Catalytic pyrolysis of biomass

The fixed-bed reactor for the pyrolysis of Yunnan pine was custom designed for this research. The furnace was heated electrically, and the temperature was measured using a thermocouple located inside the furnace. A schematic diagram of the fixed-bed reactor is shown in Fig. 1. The pyrolysis reaction was conducted in a reactor with a steel pipe that passed through the hole of the furnace. The top of the reactor was connected to a straight condenser. The condenser was kept at approximately 5 °C using ice water. The distance between the top of the furnace and condenser was approximately 30 cm. First, dry glass fiber was inserted into the vertically installed reactor, and this was used for loading the feedstock. Next, 1.20 g of Yunnan pine was placed into the reactor. The bottom of the reactor was linked with high-purity nitrogen, while the top of the reactor was connected with the condenser. The reactor was purged with high-purity nitrogen for 5 min before the beginning of the experiment. Then, the temperature was increased rapidly to the setting temperature, which was held for 30 min, at a heating rate of 250 °C/min. The nitrogen flow rate was 150 mL/min, the catalytic temperature was 550 °C, the pyrolysis temperature was 450 °C, and the biomass to catalyst ratio was 1:2. Then, the obtained bio-oil was dissolved using tetrahydrofuran (THF), and then analyzed. The

THF was used as a solvent for the bio-oil. The bio-char yield was determined by weighing the solid residue. The yield of the gaseous products was calculated from the difference. The following equations were used,

$$Y_L = \frac{M_1}{M_0} \times 100\% \quad (1)$$

$$Y_{S\text{-in-situ}} = \frac{M_2 - M_3}{M_0} \times 100\% \quad (2)$$

$$Y_G = 1 - Y_L - Y_S \quad (3)$$

where Y_L represents the yield of bio-oil (%), $Y_{S\text{-in-situ}}$ represents the yield of solid residue from *in situ* catalytic pyrolysis (%), Y_G represents the yield of non-condensable gas (%), M_0 represents the weight of the biomass feedstock (g), M_1 represents the weight of the liquid (g), M_2 represents the weight of the solid residue (g), and M_3 represents the weight of the initial catalyst (g).

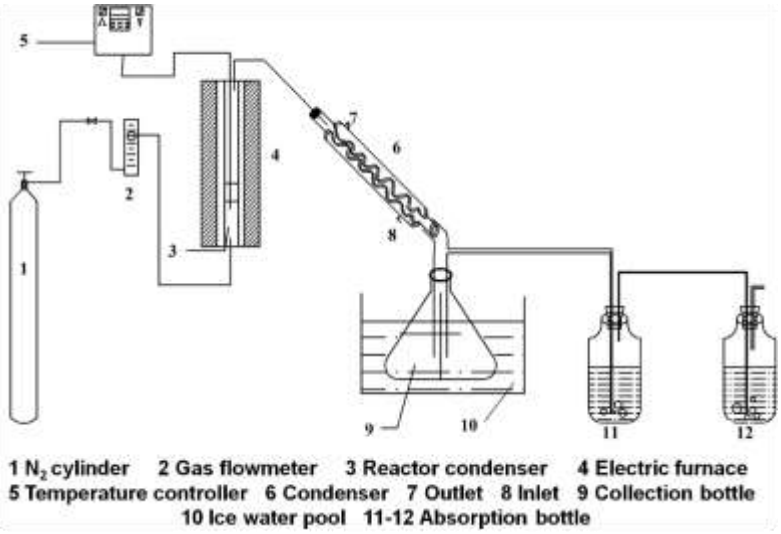

Fig. 1. Schematic diagram of the fixed-bed reactor

Characterization of the catalyst

A Magna-IR 560 ESP type Fourier transform infrared (FTIR) spectrometer (Thermo Nicolet Corporation, Massachusetts, MA, USA) with a resolution of 4 cm^{-1} and equipped with attenuated total reflection (ATR)-FTIR was used to characterize the biomass and torrefied biochars in the range of 400 cm^{-1} to 4000 cm^{-1}. The samples were placed in a potassium bromide press and scanned 32 times using the transmission method.

X-ray diffraction (XRD) data was obtained from the annealed sample surfaces using an XRD instrument (Rigaku D/max220, Tokyo, Japan). The Cu-K_α X-ray source (λ = 0.1542 nm) was operated at 40 kV and 30 mA with a Ni-filter to extract the K_α radiation. The data were collected over a scattering angle (2θ) range of 5° to 40° with a scanning speed of 2°/min. All of the measurements were conducted at room temperature and atmospheric pressure.

The elemental composition of the catalyst samples were measured by inductively coupled plasma atomic absorption spectroscopy (ICP-AES) using a Varian Vista AX CCD axial ICP-AES. For the dissolution of the solid samples, extra-purified water (5 mL) was poured into a 30 mL HDPE bottle, and 0.1g of ZSM-5 was then added. One milliliter of 4.8wt.% HF solution was added to the suspended ZSM-5 solution. After the dissolution, 1ml of 70wt.% HNO_3 was added to oxidize silicon. The solution was then brought to the 30 mL mark volume by adding extra purified water. The solution was then analyzed by ICP–AES.

The acidities of the catalysts were determined by temperature programmed desorption (TPD; Chemisorption analyser, Quantachrome Instruments, Boynton Beach, FL, USA). The catalysts (approximately 50 mg to 150 mg) were degassed by heating them to 150 °C (2.5 °C/min heating rate) with He flowing for 30 min, and then cooled to 50 °C within 60 min. The sample was allowed to absorb NH_3 gas with a 10% concentration at 50 °C for 60 min. The sample was subsequently heated to 500 °C at a heating rate of 5 °C/min with He flowing for 120 min to determine its acidity. A blank run for the catalysts, that did not absorb NH_3, was performed as a background test. Three different volumes (0.5 mL, 1 mL, and 1.5 mL) of a standard NH_3 gas (10% NH_3 and 90% He) were used to calibrate the acidity.

The C, H, N, and O contents of Yunnan pine and the products were quantified using an EA 1108 elemental analyzer (Elementar, Langenselbold, Germany). First, the C, N, and H contents were determined, and the mass fraction of O was calculated by subtracting the contents of the ash, C, N, and H from the total mass of the sample. Moreover, the water content of the bio-oil was analyzed using Karl-Fischer titration. A mixture of methanol and chloroform at a mass ratio of 3:1 was used as the titration solvent.

The higher heating values (HHVs) of the bio-char and bio-oil were calculated using Eq. 4 (Channiwala and Parikh 2002),

$$HHV(MJ/kg) = 0.3491 \times C + 1.1783 \times H + 0.1005 \times S - 0.1034 \times O - 0.0151 \times N - 0.0211 \times A \quad (4)$$

where *C*, *H*, *S*, *O*, and *N* represent the weight percentages of carbon, hydrogen, sulfur, oxygen, and nitrogen (wt.%), respectively, and *A* is the weight percent of the ash (wt.%).

The surface areas were measured using an ASAP2020 (Micrometrics, New Hampshire, USA) surface area and pore size analyzer. Prior to measurement, the samples were out-gassed at 250 °C for 12 h under vacuum. For analysis, the samples were cooled to -196 °C in a liquid nitrogen bath. Liquid nitrogen was also used as an adsorption gas. The Brunauer-Emmett-Teller (BET) surface area was calculated from the linear portion of the BET plot. The micropore volume and external surface areas were calculated using the t-plot method, and the Barrett-Joyner-Halenda(BJH) model determined the pore size distribution.

A gas chromatography-mass spectrometry (GC-MS) analysis of the bio-oil was performed with an ITQ 900 instrument (Thermo Fisher Scientific, Massachusetts, USA) using an HP-5MS (30 m × 0.25 mm × 0.25 μm) capillary chromatographic column. The injector temperature was 280 °C, and the split ratio of the carrier gas was 1:10 using high purity helium. First, the oven temperature was held at 50 °C for 5 min, and then the temperature was ramped up from 50 °C to 280 °C at 5 °C/min, which was maintained for 5 min. For the MS, the following parameters were used: an EI ionization method, ionization energy of 70 eV, and scan per second over electron range (m/z) of 30 amu to

500 amu, and an ion source temperature of 230 °C.

RESULTS AND DISCUSSION

Catalyst Characteristics

The physical properties of the HZSM-5 zeolites with different SARs, determined through XRD, N_2 physisorption, and NH_3-TPD analyses, are shown in Tables 2 and 3 and in Figs. 2 and 3.

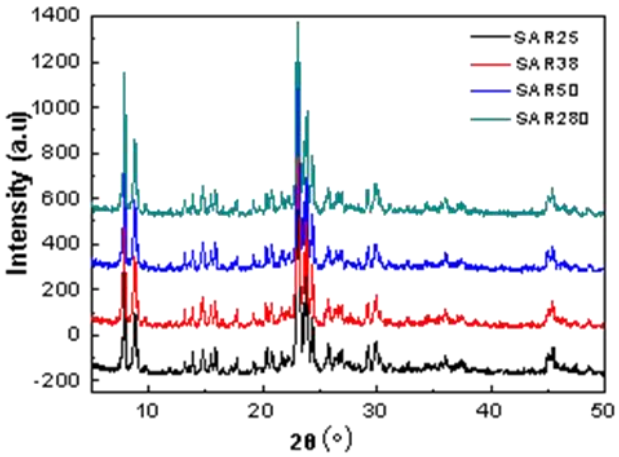

Fig. 2. XRD patterns of the HZSM-5 zeolites with various SARs

Figure 2 shows the XRD patterns of the HZSM-5 samples prepared with various SARs. The XRD characteristic peaks were at 2θ values of 8°, 9°, 23°, and 25°, which indicated that the catalyst had a special structure of zeolite molecular sieve-five (MFI) (a new topologic type of tetrahedral framework, which contains a large fraction of five-membered ring of silicon-oxygen tetrahedral structure. The framework outlines a three-dimensional system of intersecting channels defined by 10-rings of oxygen ions in all three directions. The diameters of two intersecting ten-membered ring channels are 5.1×5.5 and 5.4×5.6Å, respectively, and the size of the intersection of the two channels is 0.9 nm (Veses *et al*. 2015; Wang *et al*. 2015). The existence of these diffraction peaks showed that there was good regularity of the molecular sieve structures. All of the samples had similar XRD patterns, and there was little change in the intensity of the diffraction peaks, which indicated that the catalysts with different SARs did not destroy the molecular sieve crystal skeleton structure and there was no remarkable change in the grain size among the material.

The NH_3-TPD analysis was used to investigate the acid properties of the HZSM-5 catalysts with various SARs, and the results are shown in Fig. 3. Based on the NH_3-TPD results, the acid properties of the catalysts were determined (Table 2). The number of acid sites of the HZSM-5 gradually decreased with an increased SAR. The total acidity was 0.67 mmol/g of catalyst for SAR25 and 0.13 mmol/g of catalyst for SAR280. Meanwhile, for the elution temperature, the desorption temperature peak was at approximately 150 °C to 350 °C, which represented the weak acid sites. The peak was mainly attributable by the surface of the Si-OH zeolite. At the same time, the 350 °C to 500 °C peak represented the strong acid sites that were mainly composed of silicon hydroxyl aluminum (Si-OH-Al) zeolite, which was closely related to the content of aluminum in the skeleton (Chen *et al*. 2011).

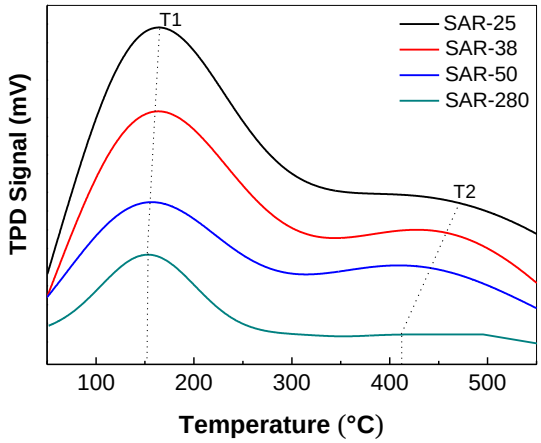

Fig. 3. NH_3-TPD profiles for the HZSM-5 zeolites with various SARs

Table 2. Physical Properties of the HZSM-5 Catalysts with Different SARs

SAR	Total Acidity (mmol/g)	Peak Temperature$_1$ (°C)	Peak Temperature $_2$ (°C)
HZSM-5 (25)	0.67	169.4	471.6
HZSM-5 (38)	0.62	165.5	457.5
HZSM-5 (50)	0.34	157.3	439.2
HZSM-5 (280)	0.13	155.5	412.5

As the SAR decreased, the desorption temperatures of T_1 and T_2 were gradually shifted to higher values. This was due to the increased Al concentration, and the strong acid sites with Si-OH-Al that gradually increased, which effectively increased the number of Brönsted acid sites and hydrophilic nature of the catalyst. This in turn influenced the total acidity of the catalyst, and the enhancement of acidity promoted the cracking reaction, which was conducive to the macromolecular cracking products and hydrogen transfer reaction. Meanwhile, as the SAR of the HZSM-5 decreased, the increased polarity of the framework helped to energetically stabilize the polar oxygenates, which are important intermediates during pyrolysis. This stabilization makes it more energy demanding to remove oxygen *via* decarbonylation, decarboxylation, or dehydration. From the point of view of deoxidation and the production of aromatic hydrocarbons, the transformation of lignin-derived oxygen-containing compounds and aromatic hydrocarbons was enhanced. This finding was in agreement with the findings of Al-Dughaither and de Lasa (2014).

Figure 4 and Table 3 show the specific surface areas and pore structures of the HZSM-5 catalysts with different SARs. The results indicated that after the subsequent exchange processing, the BET surface areas of the zeolites were between 257 m^2/g and 309 m^2/g. This was due to the impregnation process, where H atoms with a smaller radius got into the pores of the molecular sieve, and covered part of the inner surface. The specific surface areas were different, but the pore sizes were not. The materials with higher surface areas generally had slightly higher pore volumes, but overall, there was little difference in the pore volumes. It was confirmed by the nitrogen adsorption measurements that all of the samples had micro porous volumes of approximately 0.1 cm^3/g to 0.2 cm^3/g and mesoporous volumes between 0.05 cm^3/g to 0.09 cm^3/g (Table 3). Table 3 did not reveal any obvious correlation between the pore structures of the catalysts

used in this study and the SAR. These results were the same as for a previous study by Kim *et al*. (2015).

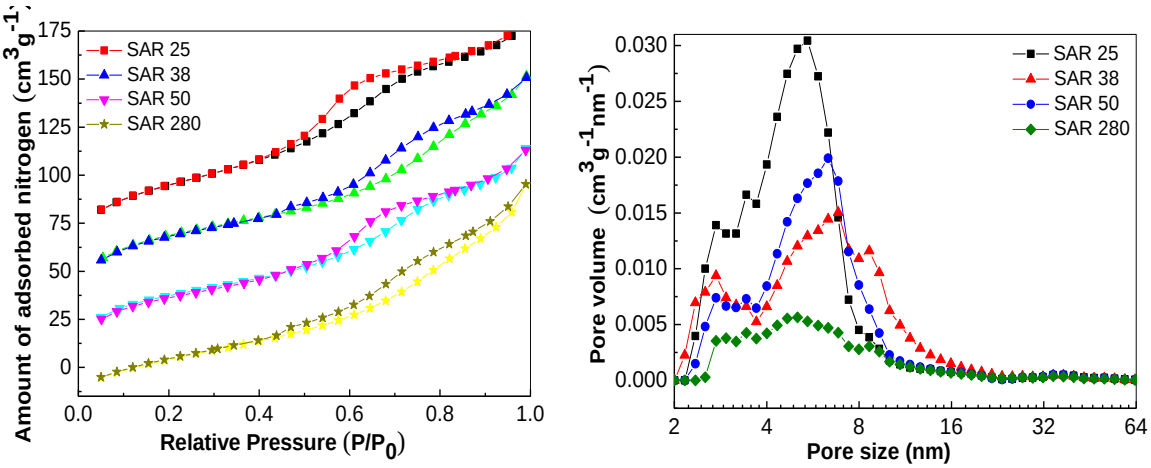

Fig. 4. Pore structure parameters of the catalysts

Table 3. Pore Structure Parameters of the HZSM-5 Catalysts with Different SARs

Sample	Si/Al	S_{BET} (m^2/g)[a]	S_{micro} (m^2/g)[b]	S_{ext} (m^2/g)[b]	V_{total} (mL/g)[c]	V_{meso} (mL/g)[d]	V_{micro} (mL/g)[b]	$D_{pore\ size}$ (nm)[a]
SAR25	25.8	308.13	148.55	159.58	0.2638	0.1969	0.07698	3.42
SAR38	37.7	312.63	174.43	136.82	0.2612	0.1759	0.09083	3.37
SAR50	48.3	284.40	154.67	121.61	0.2370	0.1639	0.08373	3.43
SAR280	282.1	257.33	135.75	121.58	0.2011	0.1495	0.0516	4.12

[a] From N_2 absorption measurement (BET method); [b] t-plot method; [c] BJH method; [d] by difference method

Figure 5 shows the FTIR spectra of HZSM-5 catalysts with different SARs.

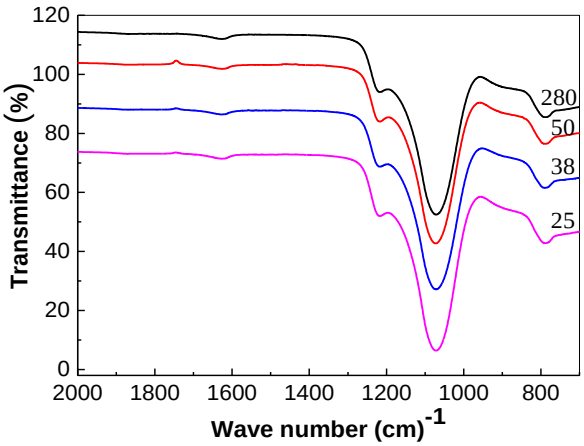

Fig. 5. FTIR spectra of the HZSM-5 catalysts with different SARs

The absorption bands near 800 cm^{-1}, 1084 cm^{-1}, and 1220 cm^{-1} were characteristic of SiO_4 tetrahedron units, which showed the internal vibration of the SiO_4/AlO_4

tetrahedral for ZSM-5, silica, and quartz. The characteristic band at 1220 cm^{-1} was the external stretching vibration, which indicated the presence of a structure that contained four chains of 5-membered rings arranged around a two-fold screw axis, such as in the ZSM-5 structure. The characteristic band at 1084 cm^{-1} was the internal asymmetric stretching vibration of the Si-O-T linkage, and the band at 800 cm^{-1} was the symmetric stretching vibration of the external linkage (Shirazi *et al*. 2008). As shown in Fig. 5, these characteristic peaks became wider and shifted towards higher wave numbers as the SAR increased, which confirmed that as the SAR decreased, the Al content increased.

Catalytic Pyrolysis of Biomass

Effect of the pyrolysis temperature

Figure 6 illustrates the effect of the pyrolysis temperature (400 °C, 450 °C, 500 °C, 550 °C, 600 °C, and 650 °C) on the aromatic selectivity of the pyrolysis products for SAR25. The experimental conditions were a feedstock particle size between approximately 0.250 mm and 0.420 mm, nitrogen flow rate of 150 mL/min, catalytic temperature of 550 °C, and biomass to catalyst ratio of 1:2 (wt.%). As shown in Fig. 6, the total aromatic selectivity (S_{BTXE}) slightly increased from 67.72% to 69% as the pyrolysis temperature increased from 400 °C to 450 °C, but as the temperature further increased, from 450 °C to 650 °C, this trend reversed.

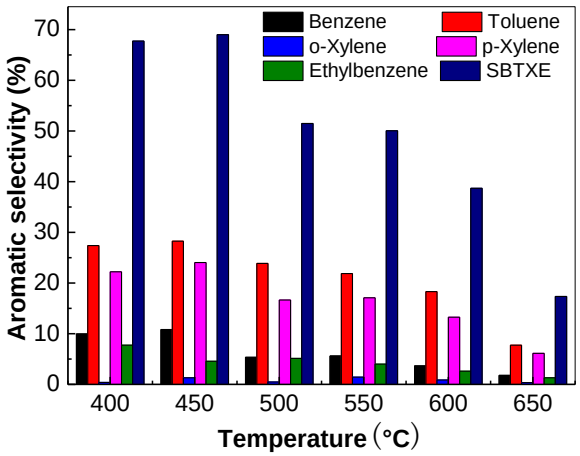

Fig. 6. Effect of the reaction temperature on the aromatic products distribution

The lowest total aromatic selectivity (17.3 wt.%) was obtained at 650 °C. This result was nearly in accordance with a previous report by Acikgoz and Kockar (2007). High temperatures inhibited the reaction because the aromatic products underwent hydrogen transfer and polymerization reactions, which are both exothermic reactions. As a result, the content of the single ring aromatic hydrocarbons was reduced, and these compounds were transformed into polycyclic aromatic hydrocarbons. The formation of polycyclic aromatic hydrocarbons at high temperatures caused deterioration of the catalyst structure, which reduced the deoxidation ability. In contrast, an increase in the pyrolysis temperature increased the yield of CO_2 and CO. The large increase of these gas contents dramatically decreased the concentration of organic vapor, and thus, decreased the production of hydrocarbons over the zeolite catalyst bed (Wang *et al*. 2014). For different reaction temperatures, the benzene, toluene, and xylene selectivities were

different. As the reaction temperature increased, the selectivities of benzene and toluene increased for 450 °C to 500 °C, then decreased for 500 °C to 650 °C. The xylene and ethyl benzene contents noticeably decreased at higher temperatures. High temperatures favored the cracking of ethyl benzene into benzene and ethylene, while at the same time, the alkylation reaction (a typical exothermic reaction) of xylene decreased. Because of the high temperatures, benzene and toluene did not easily produce an alkylation reaction and only generated more low carbon hydrocarbons, and as such, the selectivity of these compounds also decreased (Zhang *et al*. 2009). Therefore, after comprehensive considerations of the yield and selectivity of the aromatics, the optimal experimental temperature was 450 °C.

Effect of SARs on the product yield

As shown in Fig. 7, the SAR's effect on the pyrolysis products' yield was a remarkable decrease of the yield of bio-oil but the yield of bio-gas increased compared to the pyrolysis reaction without catalyst. At the same time, with an increased SAR, the liquid yield increased, while the yield of bio-gas clearly decreased. This was related to the acidity of the catalyst. The increased number of Brönsted acid sites promoted the decomposition of biomass into molecular fragments. The more acidic the surface is, the more conducive it is to the catalytic pyrolysis of biomass (Yu *et al*. 2014). Thus, when the SAR was 25, the yield of bio-oil was lower, with a higher content of gaseous products, such as H_2, CO, CO_2, CH_4, olefins, *etc*. (Huang *et al*. 2012). The effect of catalytic deoxygenation was not complete for SAR280, and the liquid phase was higher because of the weaker acidic strength.

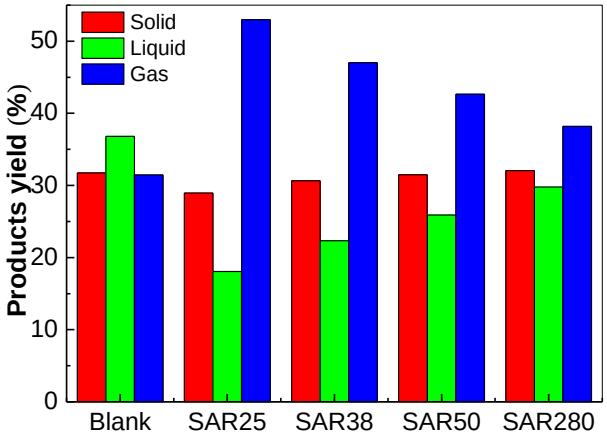

Fig. 7. Product yields from the catalytic pyrolysis of pine with different SARs

Table 4 displays the effect of the SAR on the properties of the five bio-oils. As shown in the table, the improvement to the catalytic pyrolysis vapor phase effectively improved the characteristics of the bio-oil, and the heating value increased 27.7 wt.%. As the SAR decreased, the H/C ratio and oxygen content decreased and the effect of deoxygenation was major. In addition, the calorific value increased noticeably, and the catalytic effect also increased. This was because the acidity of the catalyst was closely related to the SAR. The reaction performance depended on the number of acid centers and the acid density. With an increase of the SAR, the surface hydrophobicity of the catalyst was enhanced, the acidity of the surface was decreased, and the number of active

centers was reduced; therefore, the catalyst was less hydrophobic, which was more beneficial to the enhancement of the role of organic compounds.

Table 4. Elemental Analysis of the Different Upgraded Bio-oils

SAR	C	H	N	O[a]	H/C Mole Ratio	O/C Mole Ratio	HHV (MJ/kg)	Water Content (wt.%)
Blank	55.58	7.64	1.28	35.5	1.65	0.48	24.72	20.15
SAR25	68.97	8.26	1.12	21.65	1.44	0.24	31.55	6.75
SAR38	67.61	8.12	1.07	23.2	1.44	0.26	30.76	4.38
SAR50	65.85	8.11	1.11	24.93	1.48	0.28	29.95	2.96
SAR280	59.18	7.09	1.06	32.67	1.44	0.41	25.62	2.01

a: Calculated by difference

The surface acidity determined the number of catalytic active centers. When the hydrophobic property was poor and the HZSM-5 molecular sieve was exposed to water, the catalytic performances were reduced (Ramaiah *et al*. 2013). Therefore, the SAR280 acid center had a lower density, and the catalytic performance was weaker. The hydrophobicity of the SAR25 catalyst, which had more active centers, was poor, but the catalytic performance was better. At the same time, after the addition of the catalyst, the water content of the bio-oil increased. The catalyst provided a large number of micro pores, which was beneficial to the removal of hydrogen and oxygen; thus more pyrolysis vapor was converted into water. Moreover, the water content increased with increased SAR, and the water content clearly decreased due to the secondary cracking of the initial pyrolysis steam (Amutio *et al*. 2012).

Figure 8 displays the infrared spectrums of bio-oil obtained under different SAR. The C-O stretching vibration at about 1050 cm^{-1} indicated phenolics, alcohols, ethers, and esters were present in the bio-oil.

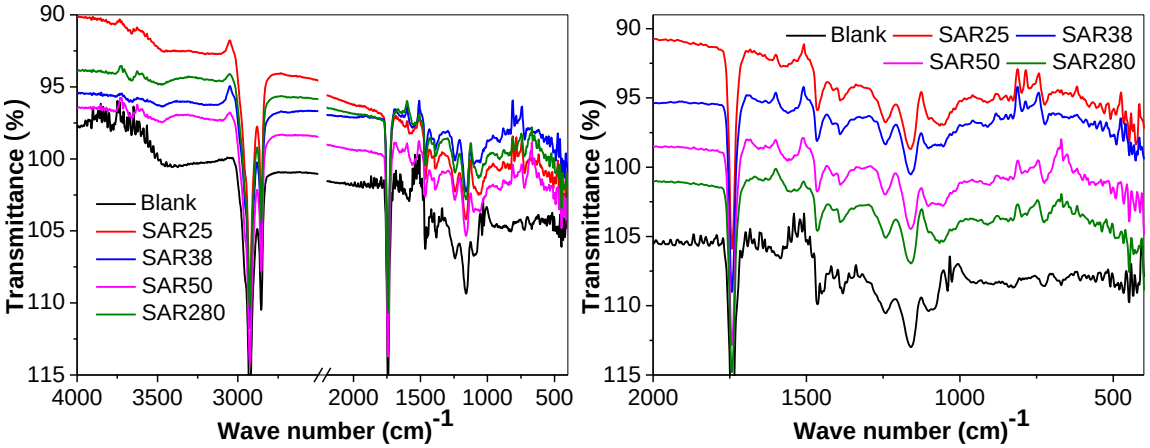

Fig. 8. FTIR spectra of the bio-oil with different SARs

The C=O bond at 1715 cm^{-1} mainly gave the evidence of carboxylic acids. The absorption peak at 2950 cm^{-1} was attributed to the C-H stretching and this demonstrated the presence of alkyl groups. The wide absorption peak between 3300 cm^{-1} and 3400 cm^{-1} was attributed to the stretching vibration of O-H, accounting for the presence of alcohols

and phenols. The signals at 1160 cm^{-1} and 1080 cm^{-1} indicate deformation vibrations of C–H bonds in guaiacyl rings and deformation vibrations of C–O bonds in secondary alcohols and aliphatic ethers, respectively. Lastly, the signal at 830 cm^{-1} is due to the substituted aromatic structure (including naphthalenes).

A comparison of the spectra revealed that the bio-oil is mainly composed of oxygen-containing compounds, such as alcohols, phenols, esters, and ketones under the conditions without the catalyst. Regarding the *ex-situ* catalytic pyrolysis upgrading processes with the HZSM-5 catalyst, the oxygen-containing functional groups (–OH , C=O, and C-O) of bio-oil decreased, and aromatic ring C-H stretching increased, which agreed with the results of GC-MS of bio-oil. That is, the products were essentially similar, and only the contents were different.

Effect of SARs on the selectivity of the aromatic products

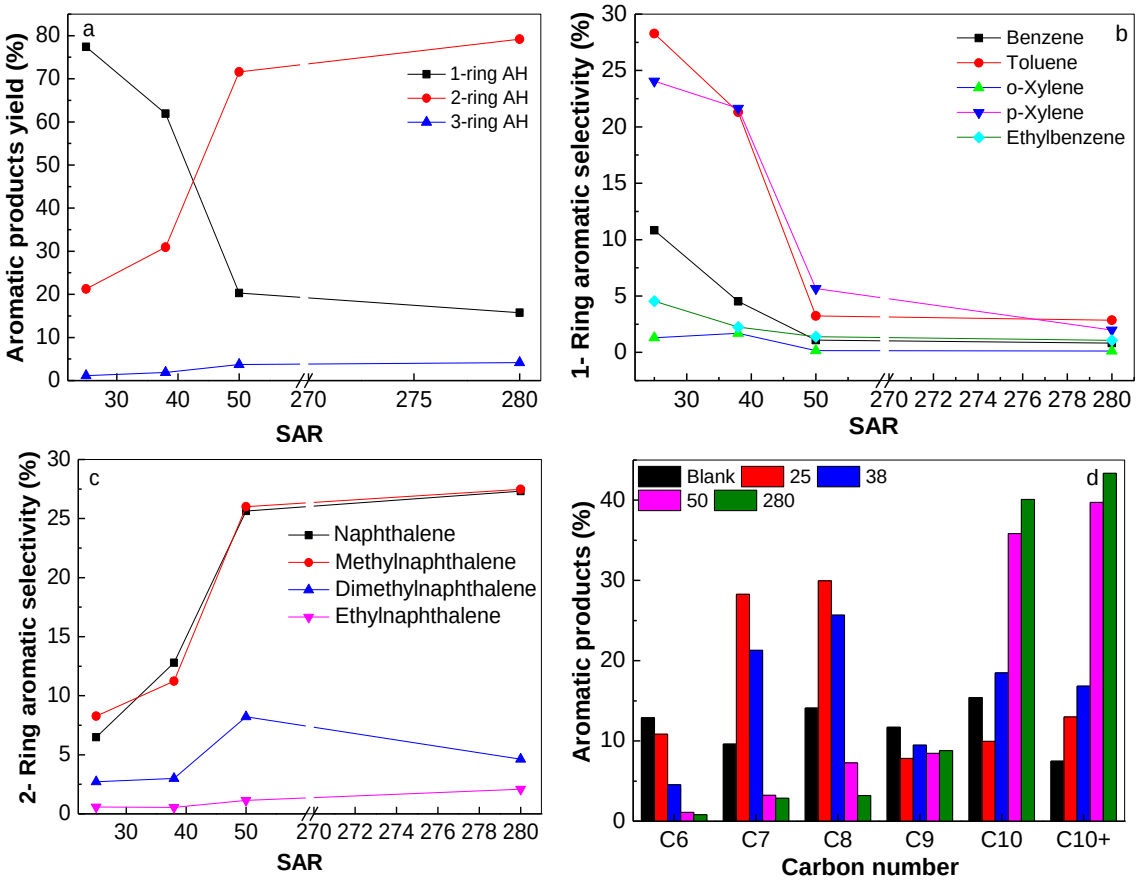

Fig. 9. Aromatic products and selectivity during vapor upgrading with ZSM-5 zeolites with different SARs; a: total aromatic products; b: 1-ring aromatic hydrocarbon (AH) selectivity; c: 2-ring AH selectivity; and d: carbon number

As the SAR increased, which corresponded to a six-fold increase in the acid density from a minimum acidity of 0.13 mmol/g to a maximum acidity of 0.67 mmol/g, the content of 1-ring aromatic hydrocarbons from the biomass pyrolysis decreased, and the content of 2- and 3-ring aromatic compounds increased (Fig. 9a). The single and double rings changed remarkably. This was because on the inside of the molecular sieve,

acid-catalyzed oxygenated compounds underwent polymerization, decarbonylation, decarboxylation, and cracking reactions. Because of the protons at the acid sites of the molecular sieve, the hydrocarbons generated a positive carbon ion and further released the β-H generating C2-C6 olefins. The olefins underwent polymerization, cyclization, and hydrogen transfer reactions, and produced aromatics. The acid dehydration capacity was enhanced, and the cracking reaction was promoted, which was conducive to the cracking of large molecular products. In addition, the Diels-Alder reaction of olefins was promoted and produced aromatics. The catalyst with a lower acid strength was not conducive to the occurrence of the hydrogen transfer reaction; thus the content of aromatics was lower (Mihalcik *et al*. 2011). The selectivity of aromatics for different SARs were different. The selectivity of 1-ring aromatics (BTX) decreased when the SAR increased. The selectivities of toluene and p-xylene in the SAR25 were the highest. The selectivity of aromatics varied with acidity. The content of BTX compounds, such as benzene, toluene, and xylene, decreased with increased SAR. The highest selectivity of BTX was obtained for SAR25 (Fig. 9b), which may have been due to the formation of toluene by the reaction of single ring and multi-substituted 1-ring aromatics that underwent a disproportionation reaction (Tsai *et al*. 1999). The increased proximity of the acid sites promoted reactions that led to a higher degree of cyclization, rather than alkyl addition and transalkylation reactions. Because p-xylene had a diameter of 0.51 nm, which was less than the average pore size of the molecular sieve (0.51 nm × 5.5 nm), the resistance to diffusion within the molecular sieve was relatively small. This resulted in a higher xylene selectivity. As shown from the selectivity of the 2-ring aromatic compounds displayed in Fig. 9c, the selectivities of naphthalene and methyl naphthalene increased with increased SAR, while the selectivity of di-methyl naphthalene was reduced and the change of ethyl naphthalene was nearly constant. Figure 9d shows the effect of the SAR on the carbon number. The selectivity of C7, C8 (benzene, toluene) in the bio-oil was higher for lower SARs, while the content of the polycyclic aromatic hydrocarbons (naphthalene, methylnaphthalene, anthracene, *etc*.) remarkably increased with higher SARs. Finally, it was interesting to note that while the mono-methylated aromatic compounds were the most selective products in each ring family for all of the ZSM-5 catalysts tested, the increase of the SAR resulted in benzene, naphthalene, and anthracene selectivities of 92.4, 76.2, and 53.8 wt.%, respectively. The substituted aromatic content increased with an increase in the SAR, and the non-substituted aromatic content decreased. This result was nearly in accordance with a previous report by Engtrakul *et al*. (2016).

Effect of addition method on the selectivity of aromatic products

To investigate the effect of the addition method on the aromatic hydrocarbons of biomass catalytic pyrolysis, the catalysts were added by *in-situ* and *ex-situ* methods. As shown in Fig. 10, it was found that the content of solid residue was not very different, and the mixed pyrolysis solid residues was slightly higher for *in-situ* catalytic pyrolysis than for the *ex situ* catalytic pyrolysis. These results agreed with the results of Wang *et al*. (2012). For *in-situ* catalytic pyrolysis, the lower mass transfer rates, as previously described, had enhanced the coke-forming reactions, which would explain the higher residue yield. For *ex-situ* catalytic pyrolysis, large amounts of carbon were deposited as pyrolysis char. Moreover, the pyrolysis vapor was in direct contact with the preheated catalyst without the limitation of heat transfer (Wang *et al*. 2014).

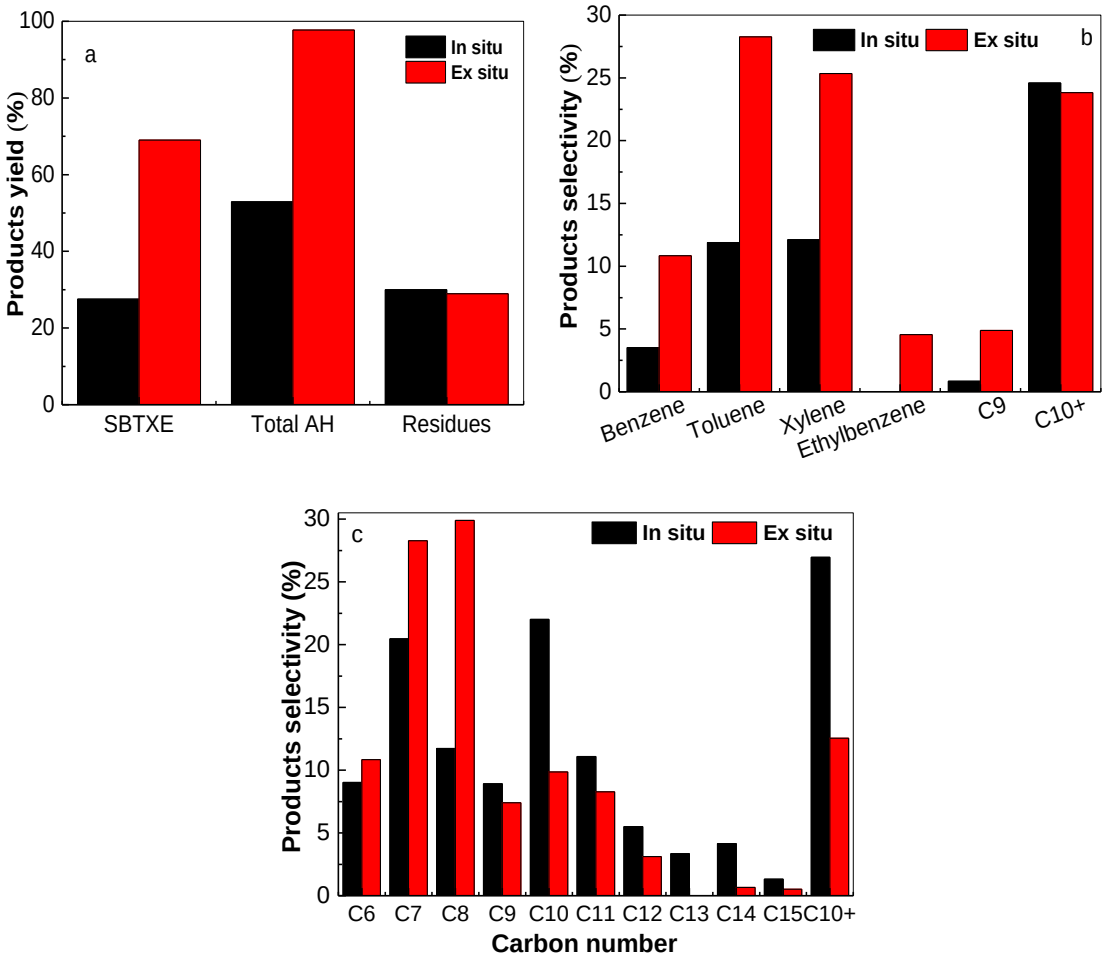

Fig. 10. (a) Aromatic products distribution, (b) selectivity, and (c) carbon number for *in situ* and *ex situ* catalytic pyrolysis

The composition and selectivity of the bio-oil exhibited large differences for *in-situ* and *ex-situ* catalytic pyrolysis. The selectivities of benzene, toluene, xylene, and other single ring aromatics were larger in *ex-situ* catalytic pyrolysis. The S_{BTXE} was 69 wt.% for *ex-situ* catalytic pyrolysis, which was much higher compared to the 27.51 wt.% for *in-situ* catalytic pyrolysis. However, *in-situ* catalytic pyrolysis generated more derivatives and C10+ polyaromatics due to the different solid particle sizes and heat transfer limitations. The formation of higher oxygenated products and faster desorption of aromatic hydrocarbon products from the acid sites of the zeolite catalyst during *ex-situ* catalytic pyrolysis might explain the lower yields of polyaromatics compared with *in-situ* catalytic pyrolysis (Nguyen *et al*. 2013). The small molecule olefins had no time to reorganize to produce large aromatic molecules because the generated pyrolysis gas mixed with the purge gas as it reformed, which resulted in pyrolytic vapor dilution, and there was also short contact time with the catalyst. This resulted in a decrease in the content of polyaromatics from *in-situ* catalytic pyrolysis. As a result of the suppressed mass transfer, monocyclic aromatics had more readily methylated and oligomerized to larger aromatics during *in-situ* pyrolysis.

Effect of catalyst amount on the selectivity of aromatic products

Biomass to catalyst ratios of 1:1, 1:2, 1:3, and 1:5 were used to investigate the effect of catalyst amount on the performance of *ex-situ* pyrolysis. Figure 11 shows the aromatic selectivity as a function of the biomass to catalyst ratios. With an increase in the amount of catalyst, the selectivities of benzene, toluene, and S_{BTXE} increased slightly. The selectivities of naphthalene and its derivatives also slightly increased, but the difference was not remarkable. With increased proportions of the catalyst, the volatile compounds content of the biomass was exposed to the catalyst with a greater probability, which increased the probability of the formation of aromatic compounds. However, when the amount of catalyst was further increased, secondary cracking on the catalyst surface took place, *i.e.*, the condensation of single aromatic rings occurred, which formed polyaromatic compounds. At the same time, because of the bio-oil covering the catalyst surface, the yield of bio-oil decreased. However, the amount of catalyst did not remarkably change the selectivity of the aromatics, which was consistent with the results of previous reports (Wang *et al*. 2012; Vichaphund *et al*. 2014).

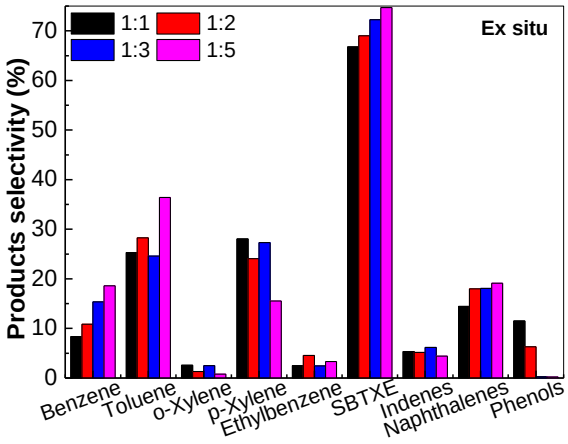

Fig. 11. Effect of the biomass to catalyst ratio on the products distribution

Effect of catalyst regeneration

Figure 12 shows the selectivity of bio-oil with a catalyst used multiple times. As shown in Fig. 12 and Table 5, after the third round with the same catalyst, the BTXE selectivity fell to 43.4 wt.%, which was lower compared with the 69 wt.% from the first round. The phenolic and oxygen-containing compounds and oxygen content all increased, which was associated with the coking and deactivation of the catalyst. The residual carbon remained on the catalyst activity center that resulted in the reduction of catalyst activity, and it reduced the selectivity of the monocyclic aromatics, which was consistent with the results given in Table 5. As the number of times the catalyst was used increased, the carbon content gradually reduced, the oxygen content increased in the bio-oil, and the calorific value was reduced from 31.6 MJ/kg to 27.9 MJ/kg. However, the element contents of the bio-oil for the regenerated catalyst were similar to that of the first use of the catalyst. This demonstrated that the activity of the catalyst was essentially fully recovered after regeneration, thus the catalyst had a better stability.

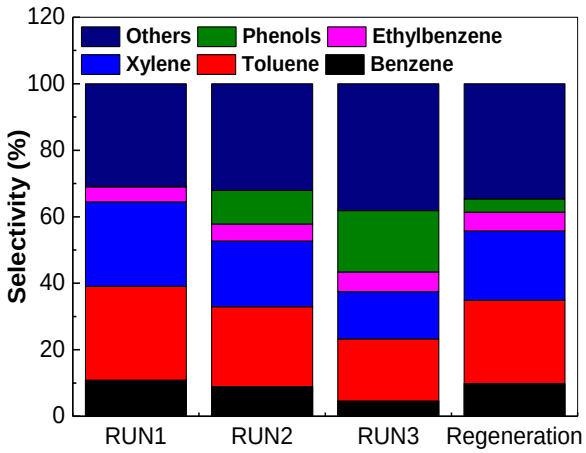

Fig. 12. Selectivity of the bio-oil when a catalyst was used numerous times

Table 5. Element Analysis of the Different Upgraded Bio-oils with Multiple Runs of a Catalyst

Samples	C	H	N	O[a]	H/C Mole Ratio	O/C Mole Ratio	HHV (MJ/kg)
Blank	55.58	7.64	1.28	35.50	1.65	0.48	24.72
RUN1	68.97	8.26	1.12	21.65	1.44	0.24	31.55
RUN2	65.82	8.27	1.20	24.71	1.51	0.28	30.17
RUN3	61.26	8.14	1.15	29.45	1.59	0.36	27.93
Regeneration	64.07	8.12	1.06	26.75	1.52	0.31	29.17

a: By difference

CONCLUSIONS

1. As the SAR increased, the catalyst pore volume and average pore diameter increased, the total acidity and catalytic activity decreased, and the yield of bio-oil increased. The gas yield, calorific value, and moisture content were reduced.
2. As the SAR decreased, the content of BTXE increased noticeably, and the content of condensed aromatics decreased. At the same time, different compounds displayed different selectivities. The benzene, toluene, and xylene selectivities increased noticeably, and the naphthalene and methylnaphthalene selectivities decreased. An increase in the SAR increased the substituted aromatic content, but decreased the unsubstituted aromatic content.
3. The *ex-situ* catalytic pyrolysis with a higher content of aromatic hydrocarbons displayed better selectivity of single ring aromatic hydrocarbons than *in-situ* catalytic pyrolysis. In addition, the solids yield and selectivity of polycyclic aromatic hydrocarbons in *ex-situ* catalytic pyrolysis were lower than in *in-situ* catalytic pyrolysis.
4. When the pyrolysis temperature was 450 °C, the catalytic temperature was 550 °C, the nitrogen flow rate was 150 mL/min, and the SAR was 25, the content of the bio-oil was the lowest, and the non-condensable gases content was the highest. At the

same time, the calorific value increased 27.7 wt.% and the water content of the bio-oil was 6.8 wt.%, and the single ring aromatics BTXE selectivity was highest at 69 wt.%.

ACKNOWLEDGMENTS

This work was supported by the Key Laboratory of Bio-based Material Science & Technology (Northeast Forestry University), Ministry of Education (Grant No. SWZCL2016-08), the National Natural Science Foundation of China (31670599), the 948 project (Grant No. 2013-4-08) in the State Forestry Administration, the Special Fund for Renewable Energy Development in the Yunnan Province (Yunnan Finance Industry No. (2015) 86), the Yunnan Provincial Department of Education Major Project of Scientific Research Foundation (Grant No. ZD2014012).

REFERENCES CITED

Acikgoz, C., and Kockar, O. M. (2007). "Flash pyrolysis of linseed (*Linum usitatissimum* L.) for production of liquid fuels," *J. Anal. Appl. Pyrol.* 78(2), 406-412. DOI: 10.1016/j.jaap.2006.10.007

Al-Dughaither, A. S., and de Lasa, H. (2014). "HZSM-5 zeolites with different SiO_2/Al_2O_3 ratios. Characterization and NH_3 desorption kinetics," *Ind. Eng. Chem. Res.* 53(40), 15303-15316. DOI: 10.1021/ie4039532

Amutio, M., Lopez, G., Artetxe, M., Elordi, G., Olazar, M., and Bilbao, J. (2012). "Influence of temperature on biomass pyrolysis in a conical spouted bed reactor," *Resour. Conserv. Recy.* 59, 23-31. DOI: 10.1016/j.resconrec.2011.04.002

ASTM E871 (1982). "Standard test method for moisture analysis of particulate wood fuels," ASTM International, West Conshohocken, USA

ASTM E 872(1998). "Test method for volatile matter in the analysis of particulate wood fuels," ASTM International, West Conshohocken, USA.

ASTM E1755 (2001). "Standard test method for ash in biomass," ASTM International, West Conshohocken, USA.

Carlson, T. R., Tompsett, G. A., Conner, W. C., and Huber, G. W. (2009). "Aromatic production from catalytic fast pyrolysis of biomass-derived feedstocks," *Top. Catal.* 52(3), 241-252. DOI: 10.1007/s11244-008-9160-6

Channiwala, S. A., and Parikh, P. P. (2002). "A unified correlation for estimating HHV of solid, liquid and gaseous fuels," *Fuel* 81(8), 1051-1063. DOI: 10.1016/S0016-2361(01)00131-4

Chen, X. Q., Wang, Z. M., and Xiao, J. X. (2011). "*In-situ* crystallization of ZSM-5 zeolite and catalytic cracking performance for naphtha," *Chemical Reaction Engineering and Technology* 27(6), 481-487.

Foster, A. J., Jae, J., Cheng, Y. T., Huber, G. W., and Lobo, R. F. (2012). "Optimizing the aromatic yield and distribution from catalytic fast pyrolysis of biomass over ZSM-5," *Appl. Catal. A-Gen.* 423, 154-161. DOI: 10.1016/j.apcata.2012.02.030

Haw, J. F. (2002). "Zeolite acid strength and reaction mechanisms in catalysis," *Phys. Chem. Chem. Phys.* 4(22), 5431-5441. DOI: 10.1039/B206483A

Huang, W., Gong, F., Fan, M., Zhai, Q., Hong, C., and Li, Q. (2012). "Production of light olefins by catalytic conversion of lignocellulosic biomass with HZSM-5 zeolite

impregnated with 6 wt.% lanthanum," *Bioresource Technol.* 121, 248-255. DOI: 10.1016/j.biortech.2012.05.141

Huber, G. W., Iborra, S., and Corma, A. (2006). "Synthesis of transportation fuels from biomass: Chemistry, catalysts, and engineering," *Chem. Rev.* 106(9), 4044-4098. DOI: 10.1021/cr068360d

Jae, J., Coolman, R., Mountziaris, T. J., and Huber, G. W. (2014). "Catalytic fast pyrolysis of lignocellulosic biomass in a process development unit with continual catalyst addition and removal," *Chem. Eng. Sci.* 108, 33-46. DOI: 10.1016/j.ces.2013.12.023

Kim, J. -Y., Lee, J. H., Park, J., Kim, J. K., An, D., Song, I. K., and Choi, J. W. (2015). "Catalytic pyrolysis of lignin over HZSM-5 catalysts: Effect of various parameters on the production of aromatic hydrocarbon," *J. Anal. Appl. Pyrol.* 114, 273-280. DOI: 10.1016/j.jaap.2015.06.007

Kunkes, E. L., Simonetti, D. A., West, R. M., Serrano-Ruiz, J. C., Gärtner, C. A., and Dumesic, J. A. (2008). "Catalytic conversion of biomass to monofunctional hydrocarbons and targeted liquid-fuel classes," *Science.* 322(5900), 417-421. DOI: 10.1126/science.1159210

Mihalcik, D. J., Mullen, C. A., and Boateng, A. A. (2011). "Screening acidic zeolites for catalytic fast pyrolysis of biomass and its components," *J. Anal. Appl. Pyrol.* 92(1), 224-232. DOI: 10.1016/j.jaap.2011.06.001

Mukarakate, C., Watson, M. J., ten Dam, J., Baucherel, X., Budhi, S., Yung, M. M., and Nimlos, M. R. (2014). "Upgrading biomass pyrolysis vapors over β-zeolites: Role of silica-to-alumina ratio," *Green Chem*. 16(12), 4891-4905. DOI: 10.1039/C4GC01425A.

Murata, K., Liu, Y., Inaba, M., and Takahara, I. (2012). "Catalytic fast pyrolysis of jatropha wastes," *J. Anal. Appl. Pyrol*. 94, 75-82. DOI: 10.1016/j.jaap.2011.11.008

Nguyen, T. S., Zabeti, M., Lefferts, L., Brem, G., and Seshan, K. (2013). "Catalytic upgrading of biomass pyrolysis vapours using faujasite zeolite catalysts," *Biomass Bioenerg.* 48, 100-110. DOI: 10.1016/j.biombioe.2012.10.024

Ramaiah, K. P., Satyasri, D., Sridhar, S., and Krishnaiah, A. (2013). "Removal of hazardous chlorinated VOCs from aqueous solutions using novel ZSM-5 loaded PDMS/PVDF composite membrane consisting of three hydrophobic layers," *J. Hazard. Mater.* 261, 362-371. DOI: 10.1016/j.jhazmat.2013.07.048

Shen, D., Zhao, J., and Xiao, R. (2016). "Catalytic transformation of lignin to aromatic hydrocarbons over solid-acid catalyst: Effect of lignin sources and catalyst species," *Energ Convers Manage* 124, 61-72.DOI: 10.1016/j.enconman.2016.06.067

Shirazi, L., Jamshidi, E., and Ghasemi, M. R. (2008). "The effect of Si/Al ratio of ZSM-5 zeolite on its morphology, acidity and crystal size," *Cryst. Res. Technol.* 43(12), 1300-1306. DOI: 10.1002/crat.200800149

Sluiter, A., Hames, B., Ruiz, R., Scarlata, C., Sluiter, J., Templeton, D., and Crocker, D. (2008). *Determination of Structural Carbohydrates and Lignin in Biomass* (NREL/TP-510-42618), U. S. Department of Agriculture National Renewable Energy Laboratory, Golden, CO, USA.

Tsai, T. -C., Liu, S.-B., and Wang, I. (1999). "Disproportionation and transalkylation of alkylbenzenes over zeolite catalysts," *Appl. Catal. A-Gen.* 181(2), 355-398. DOI: 10.1016/S0926-860X(98)00396-2

Vichaphund, S., Aht-ong, D., Sricharoenchaikul, V., and Atong, D. (2014). "Catalytic upgrading pyrolysis vapors of Jatropha waste using metal promoted ZSM-5 catalysts:

An analytical PY-GC/MS," *Renew. Energ.* 65, 70-77. DOI: 10.1016/j.renene.2013.07.016

Veses, A., Puértolas, B., Callén, M. S., and García, T. (2015). "Catalytic upgrading of biomass derived pyrolysis vapors over metal-loaded ZSM-5 zeolites: Effect of different metal cations on the bio-oil final properties," *Micropor. Mesopor. Mat.* 209, 189-196. DOI: 10.1016/j.micromeso.2015.01.012

Wang, K., Johnston, P. A., and Brown, R. C. (2014). "Comparison of *in-situ* and *ex-situ* catalytic pyrolysis in a micro-reactor system," *Bioresource Technol.* 173, 124-131. DOI: 10.1016/j.biortech.2014.09.097

Wang, L., Lei, H., Ren, S., Bu, Q., Liang, J., Wei, Y., Liu, Y., Lee, G. -S., Chen, S., Tang, J., *et al*. (2012). "Aromatics and phenols from catalytic pyrolysis of Douglas fir pellets in microwave with ZSM-5 as a catalyst," *J. Anal. Appl. Pyrol.* 98, 194-200. DOI: 10.1016/j.jaap.2012.08.002

Wang, Z., Li, C., Cho, H. J., Kung, S.-C., Snyder, M. A., and Fan, W. (2015). "Direct, single-step synthesis of hierarchical zeolites without secondary templating," *J. Mater. Chem. A* 3(3), 1298-1305. DOI: 10.1039/C4TA05031B

Wei, L., Dong, Y., and Zhou, G. (2011). "Catalytic performance of modified HZSM-5 on alkylation of phenol with isopropanol," in: *International Conference on Materials for Renewable Energy & Environment (ICMREE)*, 2, Shanghai, China, pp. 1976-1978. DOI: 10.1109/ICMREE.2011.5930725

Yu, N., Cai, Y., Li, X., Fan, Y., Yin, H., and Zhang, R. (2014). "Catalytic pyrolysis of rape straw for upgraded bio-oil production using HZSM-5 zeolite," *Transactions of the CSAE* 30(15), 264-271. DOI: 10.3969/j.issn.1002-6819.2014.15.034

Zhang, H., Xiao, R., Huang, H., and Xiao, G. (2009). "Comparison of non-catalytic and catalytic fast pyrolysis of corncob in a fluidized bed reactor," *Bioresource Technol.* 100(3), 1428-1434. DOI: 10.1016/j.biortech.2008.08.031

Zhang, H., Xiao, R., Jin, B., Shen, D., Chen, R., and Xiao, G. (2013). "Catalytic fast pyrolysis of straw biomass in an internally interconnected fluidized bed to produce aromatics and olefins: Effect of different catalysts," *Bioresource Technol.* 137, 82-87. DOI: 10.1016/j.biortech.2013.03.031

Article submitted: April 11, 2017; Peer review completed: July 24, 2017; Revised version received and accepted: September 16, 2017; Published: September 21, 2017.
DOI: 10.15376/biores.12.4.8286-8305